

Characterization and biodegradation of ternary blends of lignosulfonate/synthetic zeolite/polyvinylpyrrolidone for agricultural chemistry

Citation

JULINOVÁ, Markéta, Ludmila VAŇHAROVÁ, Dagmar ŠAŠINKOVÁ, Alena KALEDOVÁ, and Iva BUREŠOVÁ. Characterization and biodegradation of ternary blends of lignosulfonate/synthetic zeolite/polyvinylpyrrolidone for agricultural chemistry. *International Journal of Biological Macromolecules* [online]. vol. 213, Elsevier, 2022, p. 110 - 122 [cit. 2023-07-20]. ISSN 0141-8130. Available at <https://www.sciencedirect.com/science/article/pii/S0141813022011370>

DOI

<https://doi.org/10.1016/j.ijbiomac.2022.05.153>

Permanent link

<https://publikace.k.utb.cz/handle/10563/1011001>

This document is the Accepted Manuscript version of the article that can be shared via institutional repository.

Characterization and biodegradation of ternary blends of lignosulfonate/ synthetic zeolite/polyvinylpyrrolidone for agricultural chemistry

Markéta Julinová^{a,*}, Ludmila Vanharová^a, Dagmar Šašinková^a, Alena Kalendová^b, Iva Burešová^c

^a Department of Environmental Protection Engineering, Faculty of Technology, Tomas Bata University in Zlín, Nad Ovšírnou 3685, 760 01 Zlín, Czech Republic

^b Department of Polymer Engineering Faculty of Technology, Tomas Bata University in Zlín, Vavreškova 275, 762 72 Zlín, Czech Republic

^c Department of Food Technology, Faculty of Technology, Tomas Bata University in Zlín, Mostní 5139, 760 01 Zlín, Czech Republic

* Corresponding author. E-mail address: julinova@utb.cz (M. Julinova).

ABSTRACT

This study investigates novel ternary polymer blends based on polyvinylpyrrolidone (PVP) as the matrix in combination with lignosulfonate and synthetic zeolite. The blends were prepared by the casting method, and their properties were analysed by various techniques, i.e. FTIR analysis, differential scanning calorimetry and thermogravimetric analysis, including tests for water solubility and uptake, and determination of adhesion and hardness. The biodegradation of the blends in soil was also evaluated, and an experiment was conducted on plant growth (*Sinapis alba*). Optical microscopy showed that particles of the synthetic zeolite were relatively evenly distributed in the polymer matrix, forming random networks therein. The FTIR spectra for the blends proved that hydrogen bonding interactions had occurred between the PVP/synthetic zeolite and PVP/lignosulfonate. DSC analysis confirmed the good miscibility of the PVP and lignosulfonate. TGA results indicated that the thermal stability of the PVP was maintained. Lignosulfonate had the effect of reducing the adhesion of the blends. However, it was revealed that effect depends greatly on the presence of zeolite and the concentration of lignosulfonate. The obtained results showed that the optimal composition of the blend is 2.5 wt% of zeolite and 5 wt% of lignosulfonate into the PVP. Its water solubility and uptake was satisfactory from the perspective of handling and further utilization. A respirometric biodegradation test confirmed that the ternary blend was environmentally friendly, in addition to which a germination experiment evidenced that the lignosulfonate and synthetic zeolite promoted the root growth and development of *S. alba*. From these findings it was concluded that the novel ternary polymer blend was applicable as either as seed carriers (in the form of seed tapes) or as a biocompatible coating to protect seeds.

Keywords: Polyvinylpyrrolidone Lignosulfonate Synthetic zeolite Soil microorganisms Adhesion *Sinapis alba*

1. Introduction

Polyvinylpyrrolidone (PVP) is an amorphous polymer soluble in water, ethanol and other predominantly polar solvents. Its molecular weight ranges from 10,000 to 2,200,000 g.mol⁻¹. PVP is amphiphilic, containing a highly polar amide group, hence its hydrophilic and polar characteristics, and non-polar methylene groups in the chain and ring, furthering its hydrophobic properties [1]. It is applied in numerous industries for its excellent physical and chemical properties, such as the chemical and food sectors, as well as agriculture [2,3]. Of great importance to the pharmaceutical industry [1] and biomedicine [4,5], it is also utilized in the production of cosmetics [6], adhesive tape, hot melt adhesive [7] and packaging materials [8,9], in addition to membranes, sensors and circuit boards [7,10,11].

It should be noted, however, that PVP is very brittle and adheres strongly to a variety of surfaces from which it cannot be easily removed, while conventional thermoplastic processing of it is also not possible. Various composites or blends of PVP with natural or synthetic additives are prepared instead to overcome such drawbacks. From an ecological aspect, suitable natural additives comprise lignin, and derivatives of the same, and zeolite.

Lignin and variations of it have the advantage of being non-toxic, commercially available and inexpensive natural resources [12-14], marking them out as profitable from a business perspective for the plastics industry. The associated cost savings also appeal to those involved in polymer chemistry [15], and Grossman and Vermerris [14] highlight other benefits, i.e. the highly aromatic structure of lignin, its capability to participate in radical-mediated cross-linking reactions and the numerous functional groups available for chemical reactions, all of which enhance the physicochemical properties of such materials. Certain blends containing lignin (or its derivatives) as a component or additive have been studied in recent years, examples include: PVP/ lignin [16]; PVP/polyvinyl alcohol/lignin [17]; polyvinyl alcohol/lignin or lignosulfonate [18-20]; polylactic acid/lignin and kraft lignin [21-23]; oxo-biodegradable polyethylene/lignin [24]; polyvinyl ace-tate/lignin [25,26]; thermoplastic starch/kraft lignin [27]; and poly (ethylene oxide)/kraft lignin [12]. The studies mentioned varied as to evaluation of the intermolecular interactions, mechanical properties, thermal stability, photostability or miscibility of the given polymer materials, and applications linked with economically viable processes with lignin.

Zeolites have a similar potential to lignin for application in polymer chemistry and the plastics industry. Crystalline microporous aluminosilicates, they consist of tetrahedral SiO₄ and AlO₄. By combining individual tetrahedra it is possible to form approximately 133 different network structures. Zeolites occur naturally, and about 40 species exist, while types are also prepared synthetically. Synthesis in the laboratory permits zeolites to be fabricated with properties tailored to specific applications [28,29]. The literature on natural or synthetic zeolites in combination with polymer materials reveals that such blends have an extremely wide range of potential uses [30-39]. Description has even been given of ternary blends [35,36,39]. For example Alver et al. [39] focused on preparing ternary composites from chitosan, PVP and zeolite. Their results showed that a combination of all the components improved the properties of the resultant material, especially in thermal stability and mechanical terms. The formation of hydrogen bonds and occurrence of electrostatic interactions were noted between the individual components. In conclusion, Alver et al. [39] positively assessed zeolites for the specific physicochemical properties they lent the material.

Although several studies on the subject of polymer/lignin or poly-mer/zeolite composites have been published, the authors were not aware of one specifically on PVP/lignin/zeolite mixtures. Having

conducted a review of the literature, the belief was that combining ligno-sulfonate and zeolite particles could have a binary effect on the properties of the PVP, provided that:

- lignin and its derivatives, which have reactive hydroxyl groups in their structure, can form a strong hydrogen bond with PVP [17], leading to modification of the physical properties of PVP itself. Concurrently, adding lignosulfonate to PVP has the potential to contribute to i) reducing the adhesion of PVP to various surfaces [40] and optimizing the brittleness of the subsequent material; ii) promoting the biodegradability of PVP-based materials in the environment [41]; iii) positively influencing the growth of agricultural crops when applying such materials as seed tapes or a biocompatible seed coating to protect the seed inside, thereby possibly aiding the germination process and improving crop yield [41,42].
- zeolites, which have a high chemical and mechanical resilience, can have a significant effect on the thermal and mechanical properties of polymer blends. Since zeolites also possess high ion-exchange capacities and relatively high specific surface areas, the possibility exists for hydrogen bonds to form with PVP [43], potentially facilitating maintenance of the thermal stability of the polymer blends, in addition to other matters [36,39].

Therefore, the authors decided to prepare blends of polyvinylpyrrolidone, lignosulfonate and synthetic zeolite in order to obtain a practical material, effectively combining the individual properties of each component in a single polymer blend for application in agrochemistry. Research encompassed the thermal and structural characteristics of samples and their biodegradation.

2. Experimental

2.1. Materials and chemicals

The following materials were utilized in the preparation of the polymer blends: polyvinylpyrrolidone (PVP; $M_w = 10,000$) was purchased from Alchimica at a purity of 98%; glycerol was supplied by the Penta company; the fillers comprised commercial calcium lignosulfo-nate and laboratory prepared synthetic zeolite.

The commercial calcium lignosulfonate (the sulphite extract of wood) in the form of Borremet CA 120 (LiS; $M_w = 24,000$) was purchased from Borregaard (Germany). According to the company's product data sheet the material is 99.7% water soluble, biodegradable, contains ca 5% Ca, 6% reducing sugars and 7% S; its specific mass is 500 kg/m^3 and pH (10% aqueous solution) 4.5 ± 0.5 .

The synthetic zeolite (Z) was supplied by J. Kattauer (Faculty of Technology, UTB Zlin, Czech Republic). It had been laboratory prepared from waste material containing kaolin (70.0-78.8% SiO_2 , 17.9-22.7% Al_2O_3 , 0.32-0.53% Fe_2O_3 , 0.25-0.30% TiO_2 ; 0.34-0.43% K_2O), and was produced by Sklopisek Strelec a.s (Czech Republic) following the extraction of foundry sand. The zeolite was processed by calcination at $750 \text{ }^\circ\text{C}$ for 6 h, the molar ratio of the reaction mixture being adjusted by sodium silicate (water glass; 31.00% SiO_2 , 10.83% Na_2O and 58.17% H_2O). The final hydrothermal treatment of the reaction mixture was carried out in a closed reaction system at $130 \text{ }^\circ\text{C}$. X-ray diffraction analysis revealed the presence of the P1 zeolite structure. The synthetic zeolite, prior to application as the filler, was crushed in a ball mill (Mill Retsch MM 301, Germany). The particle sizes of the prepared zeolite ranged from 1 to 50 pm, with water uptake at $0.86 \pm 0.02\%$ and the pH of 4% aqueous solution at 10.11.

The remainder of the chemicals employed were of analytical purity, produced or delivered by Pliva Lachema Brno (Czech Republic).

2.2. Preparation of the polymer blends by the casting method

In accordance with a previous work by the authors [44], preparation of the polymer blends adhered to a proven procedure, as given below.

A solution of PVP/glycerol and suspension of lignosulfonate/zeolite were prepared separately, and proper volumes were mixed in order to prepare individual blends by casting.

Plastification of the PVP took place in the following way. A 25% solution of PVP was prepared by dissolving of 56.7 g PVP in 180 ml of demineralized water. The solution was heated in a water bath at 80 °C for 20 min under continuous stirring at 300 rpm. Upon complete dissolution of the PVP, 6.75 ml of glycerol (15 wt% to PVP) was added into the solution and the resultant mixture underwent another 30 min of stirring at 300 rpm.

The suspension of the fillers was made in the following manner. The given weight of lignosulfonate, which varied depending on the composition of the blend (**Table 1**) - 0/2.8/5.7/8.5 g (0, 5, 10, 15 wt% to PVP), was dissolved in 20 ml of demineralized water. Once it had dissolved, 1.41 g of the synthetic zeolite (2.5 wt% to PVP) was added into the solution. The subsequent lignosulfonate/zeolite suspension was stirred continuously for 30 min at 300 rpm.

Table 1 The composition of the prepared cast blends in wt%.

Sample	PVP	Glycerol (p)	Synthetic zeolite (Z)	Lignosulfonate (LiS)	Th ^a [mm]
PVP	100	–	–	–	
pPVP	85	15	–	–	1.51 ± 0.09
pPVP/Z	82.5	15	2.5	–	1.46 ± 0.23
pPVP/Z/ LiS 5	77.5	15	2.5	5	1.52 ± 0.07
pPVP/Z/ LiS 10	72.5	15	2.5	10	1.54 ± 0.12
pPVP/Z/ LiS 15	67.5	15	2.5	15	1.61 ± 0.21

^aTh is the thickness of the films ($n = 3$, mean values ± standard deviation).

The cast blends were prepared according to the following procedure. Polymeric solutions of the plasticized PVP and filler suspensions were mixed at the required ratios for 60 min under continuous stirring at 300 rpm. The resulting polymer blends were cast on a silicon pad (dimensions 170 x 170 mm) and dried in the air at 24.1 ± 0.7 °C and a relative humidity of $23.6 \pm 0.8\%$. The polymer blends in the form of films were generally dry enough to remove from the pad 72 h after being cast; these were reproduced in triplicates for each composition.

2.3. FTIR spectroscopy

An FTIR Nicolet iS10 device (Thermo Scientific, USA), fitted with an attenuated total reflectance (ATR) Smart MIRacle™ adapter containing a diamond crystal, was employed for FTIR analysis. Spectra were recorded over 64 scans, covering wave numbers ranging from 4000 to 500 cm^{-1} and a 4 cm^{-1} spectral resolution. The data collected were evaluated in Omnic 8 software (Thermo Scientific, USA).

2.4. Scanning electron microscopy

The morphology of the fillers and cast blends was observed by scanning electron microscopy (SEM). For this purpose the samples were mounted on carbon tape to enhance electrical conductivity. The surfaces of the blends were then studied on a scanning electron microscope (Phenom Pro X with the Pro Suite; Phenom-World BV, Eindhoven, Netherlands). The acceleration voltage was 15 kV.

2.5. Optical microscopy

This process occurred with the cast blends affixed to glass Petri dishes (9 cm in diameter), placed under an Olympus BX53 fluorescence microscope equipped with a number 8 filter (Olympus, Japan). The distribution of the filler on the surfaces was revealed by the light transmitted. The scale bar was created in cellSens Standard software (Olympus, Japan).

2.6. Differential scanning calorimetry

Differential scanning calorimetry (DSC) was measured in a Mettler Toledo DSC 1 model. Samples were placed into an aluminum cells (ca 5 mg) and scanning at a heating rate of 10 °C/min and a heating range from 0 °C to 210 °C. The DSC system was purged with nitrogen. Before the DSC scanning, all the samples were kept in desiccator at 25 °C. The transition temperatures (like T_g or T_m) for all the samples were determined from the second heating scan.

2.7. Thermogravimetric analysis (TGA)

Thermogravimetric analysis (TGA) was performed on STA 449 F1 Jupiter equipment fitted with FTIR Bruker Alpha II accessories. The range of measurement was from 30 °C to 600 °C at a heating speed of 10 °C/min. Samples were placed in corundum pans (ca 15 mg). Measurement took place in air to promote simulation of real-world conditions.

2.8. Texture profile analysis

Texture profile analysis, performed on a TA.XT plus texture analyser (Stable Micro Systems Ltd., UK), was carried out to determine the hardness and adhesion of the cast blends. All such tests were performed at room temperature. Each sample was placed on the base of the analyser. Following this, a 5-mm spherical P/5S probe began to descend towards the polymer system at the constant speed of 1.5 mm per second, and when the probe came into contact with the surface, a trigger of 2.5 g was activated, after which the probe proceeded to penetrate the material to the depth of 1.5 mm. The probe immediately returned to its original position subsequently. The positive region of the resultant graph related to the force required to penetrate the material. Hardness (N) was determined as the peak value, designated F1; see **Fig. 1**. The negative region of the graph pertained to the force required to remove the probe from the material. Adhesion (N) was determined as the peak value, designated F2. Fifteen replicates underwent each test condition in order to confirm the reproducibility of the findings. All the data presented herein are given as the mean values calculated for fifteen replicates, shown together with relevant standard deviations.

2.9. Water solubility

The solubility of the cast blends was investigated in accordance with a previous work by the authors [44]. "Dried samples cut into square pieces of dimensions 5 x 5 x 0.15 cm were added into Erlenmeyer's flasks with the appropriate amount of demineralized water. The course of dissolution by the samples, as gauged at selected intervals, was set by a modified method of chemical oxygen demand (COD) in a closed system, with adherence to the international standard colorimetric method -ISO 15705:2002 [45]; a small-scale sealed-tube approach was adopted to work out the chemical oxygen demand index. The COD was determined by applying potassium dichromate via the closed reflux method [20]. Mercuric sulphate was employed to mask chloride interference, while silver sulphate was dissolved in concentrated H₂SO₄ to act as a catalyst." Water solubility (%) was calculated by Eq. (1).

$$\text{Water solubility} = \frac{\text{COD}_0 - \text{COD}_n}{\text{COD}_0} \cdot 100 \quad (1)$$

where COD₀ represents the COD (mg g⁻¹) of the dried cast blends at the beginning of the test, and COD_n is the COD (mg g⁻¹) measured at an appropriate interval (n).

The courses over time for the water solubility (WS) of the pure PVP or prepared blends, WS = f(t), were described by regression, applying an equation for first-order kinetics by Eq. (2) [46].

$$\text{WS} = \text{WS}_\infty \cdot (1 - e^{-k \cdot t}) \quad (2)$$

where WS_∞ is the regression coefficient representing the limit value for infinite time (%), k is the constant rate (min⁻¹), and t stands for time (minutes).

2.10. Water uptake

The water uptake of the pre-dried cast blends was tested in a humidity chamber with ca 54% relative humidity (RH), with evaluation occurring by gravimetric analysis. Difference in weight was measured at specific time intervals until no further change in weight (± 0.001 g) was observed [44]. Afterwards, the extent of water uptake in per cent was calculated according to Eq. (3) below.

$$\text{Water uptake} = \frac{w_n - w_0}{w_0} \cdot 100 \quad (3)$$

where w₀ is the weight of the dried cast blends at the beginning of the experiment and w_n is weight at a selected interval (n).

2.11. Biodegradation

A closed OxiTop® Control respirometer (WTW GmbH, Germany) was used to determine the biodegradation of PVP and the blends of PVP, Z and LiS in a soil environment. The device gauges the biodegradation of organic substances in aerobic conditions based on oxygen consumption. The degree

of biodegradation was evaluated according to the BOD/COD ratio; the percentage of biodegradation was calculated by Eq. (4).

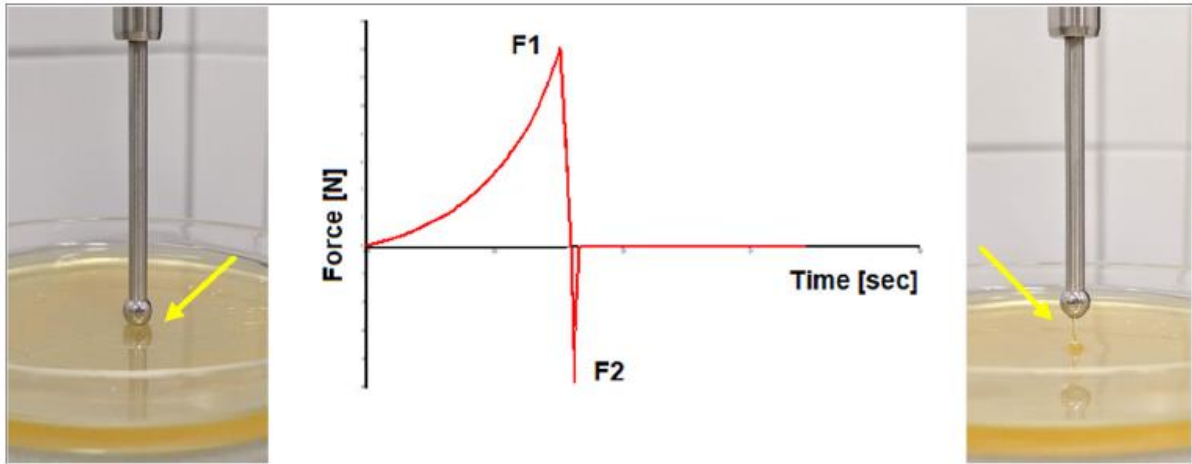


Fig. 1. Typical force vs time curve from detachment measurements, shown for the pPVP sample with 2.5% of zeolite.

The biological material comprised natural agricultural earth (Zlin, Czech Republic); 50 ± 0.1 g of the soil was weighed into a 250 ml respirometric bottle and supplemented with approximately 80 mg of the test sample (placed in the centre of the soil layer). Tests were carried out in an aerobic environment at 25 ± 1 °C under the controlled moisture of ca 55%. Concurrently, endogenous respiration was also investigated. All measurements were performed in triplicate. Determinations occurred at the commencement and close of the test, pertaining to the dry matter of the soil and its value for exchange capacity (pH_{KCl}), in order to monitor the process. Moisture was seen to be at about 55% at the beginning and end of the experiment, with values for pH_{KCl} equalling ca 6.9 and 7.2, respectively.

$$\text{Biodegradation} = \frac{(\text{BOD}_{\text{sample}} - \text{BOD}_{\text{blank}}) / w_{\text{sample}}}{\text{COD}} \cdot 100 \quad (4)$$

where $\text{BOD}_{\text{BLANK}}$ represents biological oxygen demand (mg) in the blank sample (endogenous respiration), $\text{BOD}_{\text{SAMPLE}}$ represents biological oxygen demand (mg) in a sample of the cast blend during biodegradation, COD (see Section 2.9) is the experimental determination of chemical oxygen demand (mg g^{-1}) [45] of the cast blend and w is the weight of the cast blend under study (g).

The biodegradation courses over time for the PVP and blends, $D = f(t)$, were described by regression, applying an equation for first-order kinetics of substrate degradation (Eq. (5)) [47]:

$$D = D_{\text{max}} \cdot \left[1 - e^{(-k \cdot (t - t_{\text{lag}}))} \right] \quad (5)$$

where D_{max} is the regression coefficient representing the limit value for infinite time (%), k represents the constant rate (in d^{-1}) and t_{lag} is the shift on the time axis expressing the lag phase (d).

2.12. Screening plant growth test (*Sinapis alba*)

Certified seeds of *Sinapis alba* were purchased from the Semo a.s company (Czech Republic). Preliminary incubation showed that all the seeds utilized herein showed germination rates exceeding 90%.

In accordance with the previous work by the authors [44], “the screening plant growth test [48] was performed in cultivation vessels filled with a blend of natural soil and perlite mixed in a 3:1 ratio. The blend supplemented with 5 wt% of filler was used to create seed tapes. The cast blends were attached to one other to affix seeds of *Sinapis alba* between them. These seed tapes were cut into 1 x 1 cm squares so that each square contained a seed in the middle. The samples prepared in this manner were put in the soil to a depth of about 0.5 cm below the surface. The cultivation vessels were placed in a thermostat at 25 ± 1 °C under continuous illumination of 7000 lx and 55% RH on a plastic mat of one cm height, which allowed for drainage but prevented the cultivation vessels from taking up the drainage of the surrounding cultivation vessels. This experiment ran for 12 days, and the seeds were regularly watered during this period [44,48]. No fertilizers were added during the experiment. At its close, the mean lengths of the shoots, roots and total mass of wet biomass were gauged. The elongation of the main shoot of the plant was measured every day.” All the data presented herein are given as the mean values calculated for ten replicates, shown together with relevant standard deviations.

3. Results and discussion

When designing the optimal composition of the polymer blends, organoleptic evaluation was conducted first, for instance, film formation, stickiness, flexibility and hardness.

The PVP and plasticized PVP (pPVP) were very viscous and sticky, yet it was possible to investigate the characteristics of the prepared cast polymers by the proposed technical means. The migration of glycerol to the surface of the pPVP cast blend was detected in accordance with a study Orliac et al. [49]. After adding in Z, the migration of the glycerol was suppressed and its tackiness partially reduced, such that the resultant blends could be more easily manipulated. As the level of synthetic zeolite content increased, though, the blends became brittle and cracked. Based on the organoleptic evaluation that took place, the conclusion was drawn that the most suitable filling was 2.5 wt% Z for the cast blends plasticized with 15% glycerol, this weight ratio was also applied in the preparation of blends with lignosulfonate. Blends composed solely of plasticized PVP and lignosulfonate did not form films of the required quality. When optimizing the composition of the PVP/Z/ LiS blends, the same finding was made as reported by Silva et al. [16]. LiS content in the blend at a level exceeding 15% was not suitable, since the cast products were very brittle and shattered. All the prepared cast blends of pPVP/Z/LiS with the content of LiS ranging between 5% and 15% exhibited good elastic properties and did not break. The results of the organoleptic observation thus indicated the significant influence exerted by the synthetic zeolite during preparation of the PVP and LiS blends.

A visual inspection revealed that incorporating the synthetic zeolite particles led to a change in the colour of the blends from transparent to a yellow shade. Supplementation of pPVP/Z with lignosulfonate brought about a significant change in the colour of the samples, which turned from a pale brown-red to a dark brown-red (**Fig. 3**) depending on the specific concentration.

3.1. Microscopy observations

The morphology of the lignosulfonate was studied by SEM, and micrographs are given in **Fig. 2**. The original lignosulfonate particles were quite large, spherical and hollow, as visible in the picture of the fractured sample, and had a wide distribution in size. The SEM images of the pure synthetic zeolite indicated the presence of small particles irregular in shape with a mean size of 10 to 50 μm .

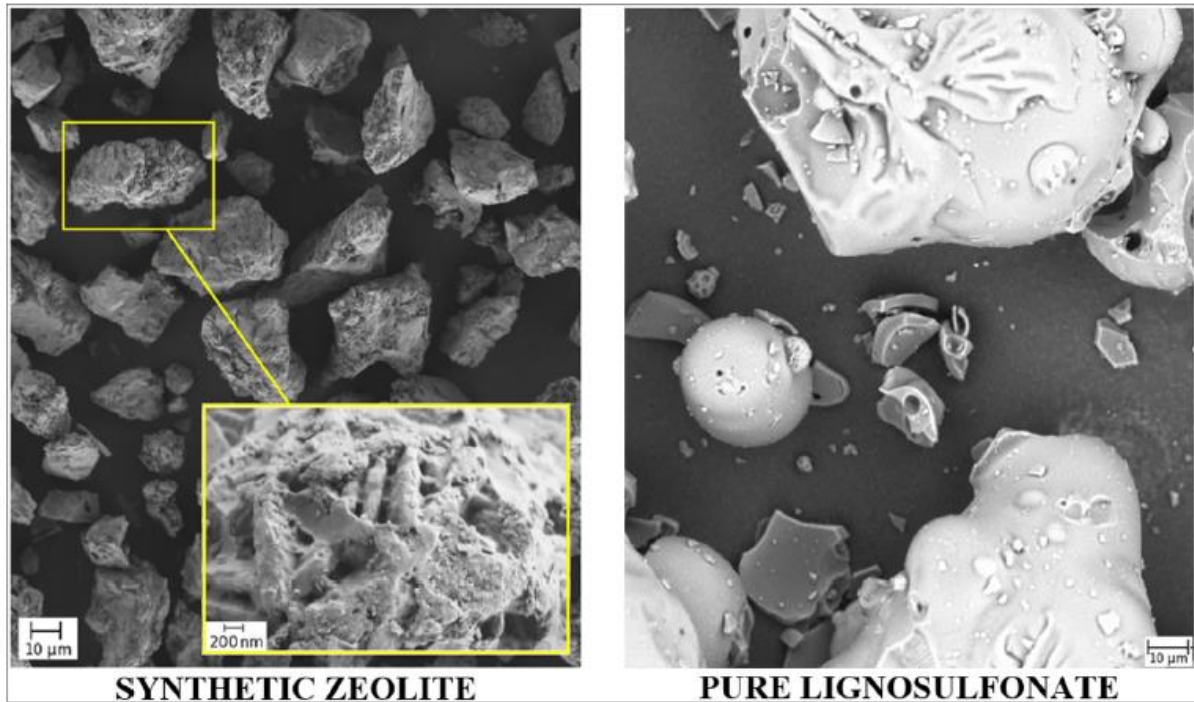


Fig. 2. SEM micrographs of synthetic zeolite and lignosulfonate particles.

Since SEM did not provide sufficient data, morphological characterization by optical microscopy took place of the PVP blends with synthetic zeolite and differing amounts of LiS. **Fig. 3** contains optical micrographs of the pure PVP, plasticized PVP and zeolite/LiS blends.

As had been anticipated, no particles were visible in the pure PVP and plasticized PVP samples (**Fig. 3A, B**), the smooth morphology evident showing just minor impurities.

The presence of the synthetic zeolite particles in the PVP blends (pPVP/Z, **Fig. 3C**) meant that their surfaces were rougher in appearance, with relatively uniform distribution of such particles throughout the matrix.

The resultant micrographs for pPVP/Z/LiS in **Fig. 3C, D, E** and **F** indicated that adding LiS had not significantly affected the distribution of zeolite particles in the polymer blends. These particles were quite evenly distributed throughout the polymer matrix and had formed random networks therein. Common phenomena seen for immiscible blends, i.e. the aggregation of large particles and lack of adhesion between the filler and matrix, were not evident, suggesting that the LiS and PVP constituted a miscible system. Such results could be attributed to intermolecular hydrogen bonds forming between

the LiS and PVP (see the FTIR analysis). Similar findings were reported by Ye et al. [18] for mixtures of poly(vinyl alcohol) with a low concentration of calcium lignosulfonate.

3.2. FTIR spectroscopy

Infrared spectroscopy was conducted to investigate the specific interactions that had occurred between the PVP and fillers. According to the literature [16,17,50], the presence of intermolecular hydrogen bonds was to be expected.

In agreement with Kubackova et al. [51], the FTIR spectra for lignosulfonate (Fig. 4A) revealed bands typically corresponding to functional groups expected in the lignin sample. The strong wide band at 3500-3100 cm^{-1} with a peak at 3339 cm^{-1} was assigned to O—H stretching vibrations, caused by the presence of alcohol and phenolic hydroxyl groups; the latter greatly affects the antioxidant properties of lignosulfonate. The adsorption band at 2939 cm^{-1} was attributed to the C—H stretching vibration of methoxyl groups, while those at 1597 cm^{-1} and 1511 cm^{-1} pertained to stretching vibrations of C—C bonds in the skeleton of aromatic rings in the calcium lignosulfonate. O—H stretching vibrations of secondary (1157 cm^{-1}) and primary alcohols (1034 cm^{-1}) were also discerned [51]. FTIR spectra for synthetic zeolite (Fig. 4B) contained a broad adsorption band at 3382 cm^{-1} relating to the stretching vibration of O—H, and the one at 1635 cm^{-1} constituted an H—O—H bending vibration. Liu et al. [52] wrote that adsorption bands at 1635 cm^{-1} and 3382 cm^{-1} indicated the vibrations of hydroxyl groups or the solid phase hydrate water in zeolite P1 channels. The band located at 980 cm^{-1} expressed the asymmetric stretch vibration of a TO_4 (T = Si or Al) tetrahedral, in addition to which symmetrical stretch vibrations of an internal tetrahedron in zeolite P1 at 742 and 693 cm^{-1} were evident [44].

The FTIR spectrum for pure PVP in Fig. 4C exhibited a broad band at ca 3600—3100 cm^{-1} assigned as O—H stretching of the hydroxyl group. The two bands at 2951 and 2886 cm^{-1} were considered to pertain to the asymmetrical and symmetrical stretching of — CH_2 groups and vibration of the aliphatic compound — CH_2 . The presence of heteroatomic molecules and carbonyl groups in the pyrrolidone ring of PVP was discerned, evidenced by the adsorption band at 1666 cm^{-1} (C—O stretching) and adsorption band at 1286 cm^{-1} (C—N stretching of the amide group). Absorption bands at 1493, 1469 and 1426 cm^{-1} were denoted as vibrations of the pyrrolidone ring. The presence of hydrogen bond interactions between the PVP and fillers was inferred from changes in the position of the adsorption band of C—O stretching, such bonding being affirmed by a shift to lower wavenumbers.

The plasticized PVP (Fig. 4D, E) exhibited a broad absorption band at 3600—3000 cm^{-1} , which was split into two distinct parts at 3370 cm^{-1} and 3305 cm^{-1} indicative of different states of adsorbed water in the system [8]. The intensity of these two bands significantly increased with the addition of glycerol, since a greater number of hydroxyl groups were present. Glycerol in the system gave rise to two significant adsorption bands at ca 1111 cm^{-1} and 1044 cm^{-1} . The shoulder-like adsorption band at 1044 cm^{-1} was associated with the overlapping stretching vibrations of a C—O linkage in C1 and C3 from the glycerol and the C—C stretching of pyrrolidone from the PVP, while the adsorption band at 1070 cm^{-1} related to overlapping stretching vibrations of C—O and C—N groups from the glycerol and PVP, respectively [8]. A shift from 1666 cm^{-1} to 1650 cm^{-1} indicated that interactions had occurred in the form of hydrogen bonds between the carbonyl group in the lactam ring and -OH groups of glycerol.

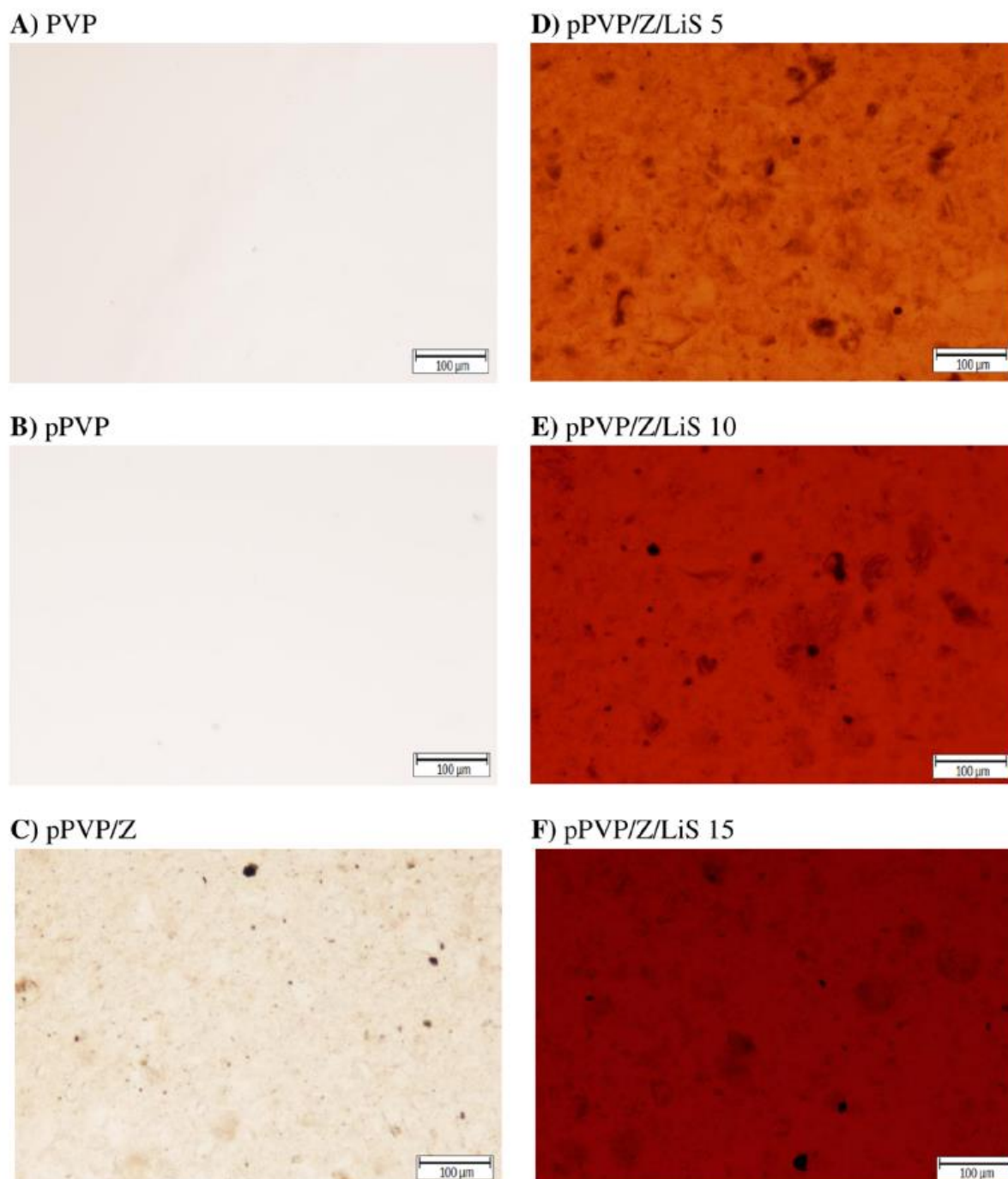


Fig. 3. Optical microscopy images of PVP, pPVP, pPVP/Z and pPVP/Z/LiS samples.

Incorporating Z and LiS in the pPVP triggered a wide band to form at $1100\text{--}880\text{ cm}^{-1}$ (Fig. 4D), which arose through the following: i) the -OH vibration of primary alcohols from lignosulfonate at 1034 cm^{-1} ; ii) the asymmetric stretch vibration of a TO_4 ($\text{T} = \text{Si}$ or Al) tetrahedral at 980 cm^{-1} ; and iii) overlapping stretching vibrations of the $\text{C}\text{--}\text{O}$ linkage in C1 and C3 from the glycerol and $\text{C}\text{--}\text{C}$ stretching of pyrrolidone from the PVP. As seen in Fig. 4E, changes in the absorption bands of the outer -OH groups at ca $3000\text{--}3600\text{ cm}^{-1}$ indicated that some of the -OH groups were involved in hydrogen bonding; probably brought about through: i) hydrogen bonding by some of the -OH groups from the synthetic

zeolite with the carbonyl group or the N atom of the PVP [43,44]; and ii) intermolecular hydrogen bonds forming between the -OH PVP and -OH of the lignosulfonate [17,50].

The results of FTIR analysis confirmed that hydrogen bonding had taken place between the PVP, lignosulfonate and zeolite, causing miscibility and enhancement of the physical properties of the cast blends.

3.3. Determination of glass transition temperature by DSC

DSC is a convenient method for determining the miscibility of polymer blends [18], whereby special intermolecular interaction between PVP and lignosulfonate is confirmed by distinct alteration in the glass transition temperature (T_g) of the PVP component.

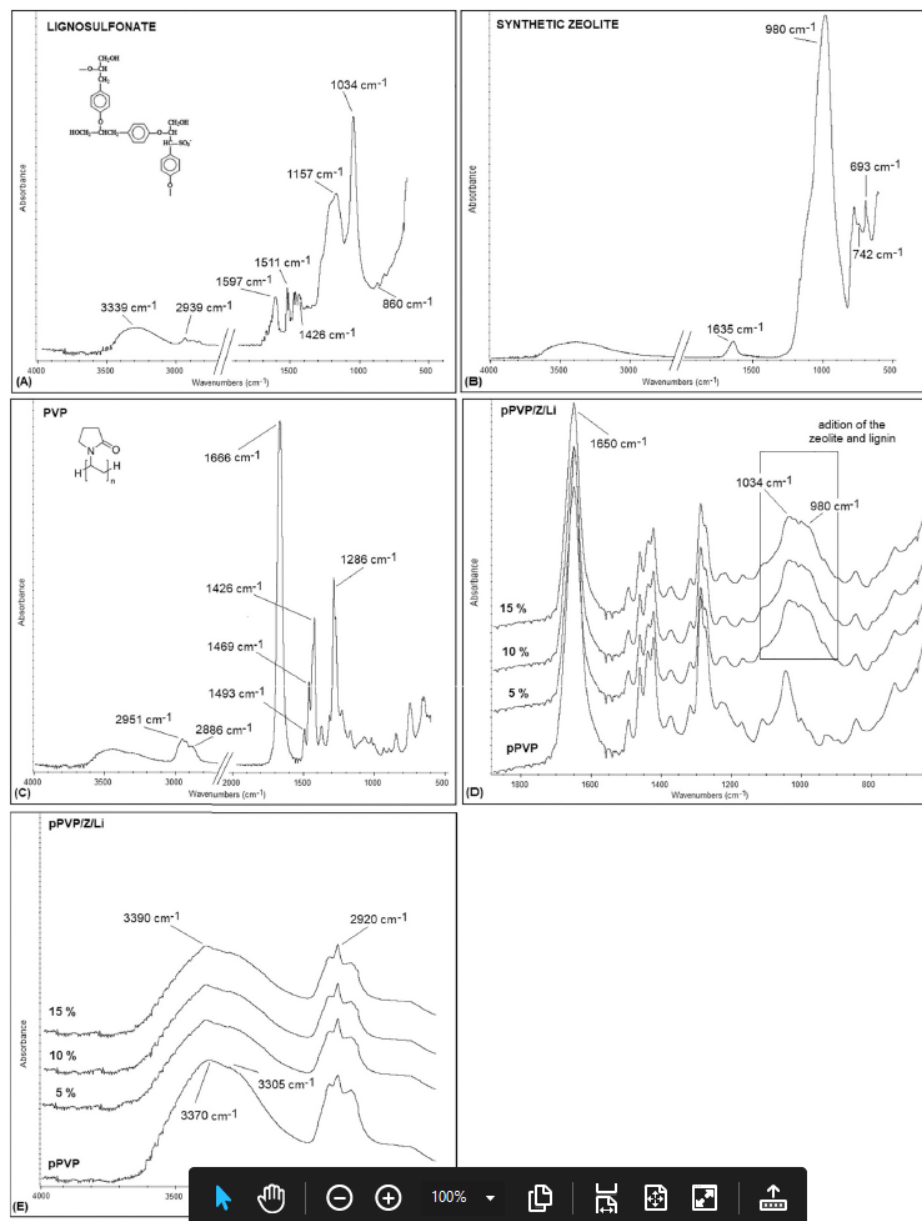


Fig. 4. FTIR spectra for the fillers and cast blends of: A) lignosulfonate; B) synthetic zeolite; C) cast PVP; D) pPVP and pPVP/Z/LiS at 600-1900 cm⁻¹; and E) pPVP and pPVP/Z/LiS at 2600-4000 cm⁻¹

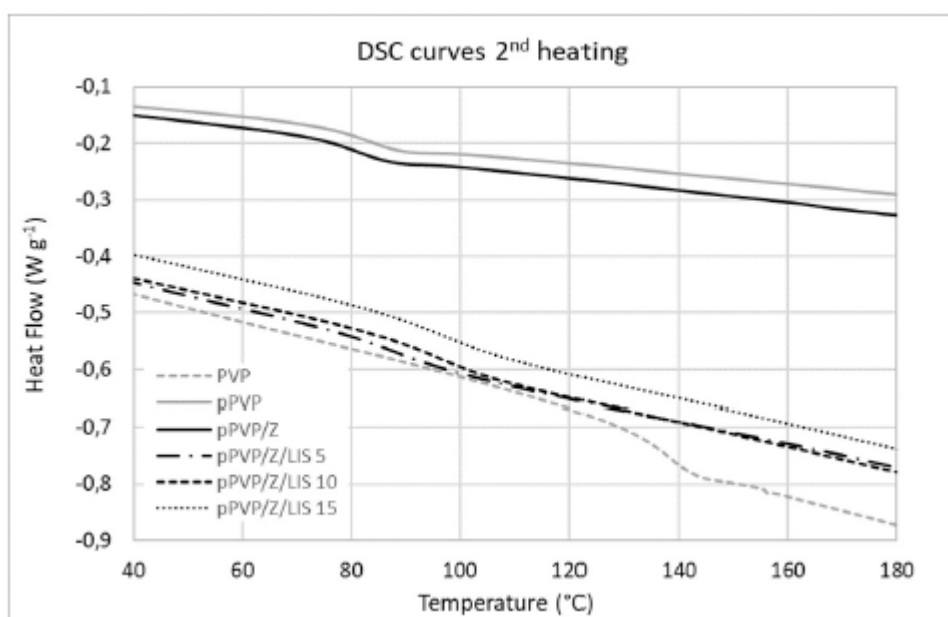


Fig. 5. DSC analysis of the cast materials of PVP, pPVP, pPVP/Z and pPVP/Z/LiS (index: 1 = first heating scan, 2 = second heating scan).

Table 2 DSC analysis (2nd heating) - evaluated data on the cast materials of PVP, pPVP, pPVP/Z and pPVP/Z/LiS.

Sample	PVP	glycerol (p)	T _g °C	T _g %
PVP	100	–	138	–
pPVP (ref.)	85	15	74	0
pPVP/Z	82.5	15	80	+8
pPVP/Z/LiS 5	77.5	15	93	+26
pPVP/Z/LiS 10	72.5	15	96	+30
pPVP/Z/LiS 15	67.5	15	98	+32

Data gathered from the DSC analysis are presented in **Fig. 5** and **Table 2**. A clear finding was that raising the extent of LiS concentration led to rise in T_g in comparison with pPVP. Samples containing 5% LiS showed change in T_g by more than 20 °C compared to pPVP. A trend was recognized for increase in the amount of LiS during the 2nd heating scan. The level of T_g rose more than 20% for the tested blend with 5% LiS, 30% for that with 10% LiS and 32% for the sample with 15% LiS, in comparison with pPVP. These results indicated that the lignosulfonate influenced the transition temperature of prepared mixtures. It could be supposed that some reactions may have occurred during the sample preparing and heating, since lignosulfonate contained numerous hydroxyl groups with the ability to interact with PVP through hydrogen bonding, thereby weakening interaction within the PVP. T_g was observed to go up in line with potential increase in concentration and strength of the hydrogen bonds. After the 2nd heating scan, the PVP mixtures were deemed to be completely miscible systems over the entire range of composition [18].

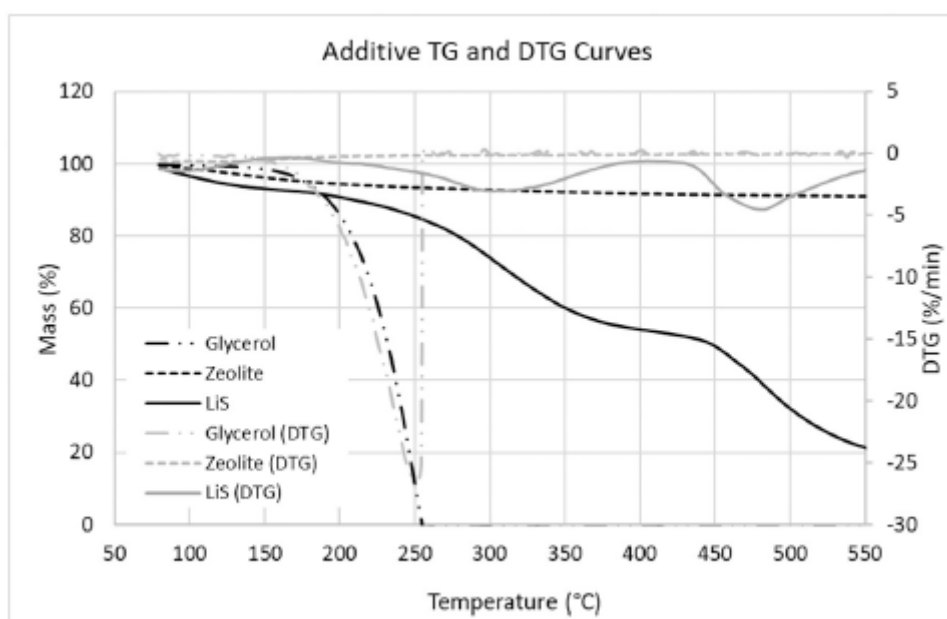


Fig. 6. TGA analysis of pure additives - TG and DTG curves for pure additives Glycerol, Zeolite, LiS.

3.4. Thermogravimetric analysis (TGA)

The performance of polymeric materials is often strongly influenced by thermal transitions within them, therefore, thermogravimetric analysis was conducted [39]. The TGA curves for the PVP mixtures in the temperature range of 50-600 °C are given in **Figs. 6 and 7**. The data is presented in **Table 3**.

Fig. 6 is focused to the pure mixture additives - glycerol, zeolite and lignosulfonate. From these results it is possible to see, that the glycerol is stable till 200 °C with maximum loss at 248 °C. Zeolite loss only 9% of weight in tested temperature range. LiS indicates 3 step degradation with maximum in 94 °C (water release), 308 °C and 481 °C with mass residual 17%.

Next **Fig. 7** offers the curves of TG and DTG (first derivation of TG) for PVP mixtures. DTG curves were obtained from the standard built-in software of the TGA instrument. These TGA results revealed that pure PVP started to lose the weight at 54 °C, with the maximum point at 82 °C, potentially connected with the release of water. The TGA for pure PVP followed a three-step form of degradation, while other compositions demonstrated a multi-step mechanism of degradation. The reference material marked as pPVP with glycerol as a plasticizer started to degrade at 121 °C, with a maximum point at 134 °C; loss in mass equalled ca 7%. Other mixtures with LiS were very similar in the first phase of degradation. Further loss in mass occurred in the region of 270-360 °C, with change in mass at 7-10%. No loss was observed in the curve for pure PVP in this region, potentially connected with the plasticizer utilized. The influence of PVP to the plasticizer degradation is evident from the obtained data. The plasticizer degrades at 248 but in combination with PVP the temperature goes up more than 50 °C. This fact could indicate the creation of hydrogen bond in the system, which could explain the improvement in the plasticizer stability. Further the LiS could degrade in this region. It was found out that with increasing LiS concentration the T_{max2} in this range fall down. Degradation was most extensive at 360-460 °C, in connection with the PVP applied. Blends with LiS exhibited a higher maximum temperature for degradation in this temperature area opposite to T_{max2} , however such change (2%) was insignificant compared to pPVP. Another finding related to change in weight, equal to 63% for pPVP and 55% for

mixtures with LiS at 10% and 15% (an improvement of 14%). A possibility was that the LiS positively influenced the main phase of such PVP degradation.

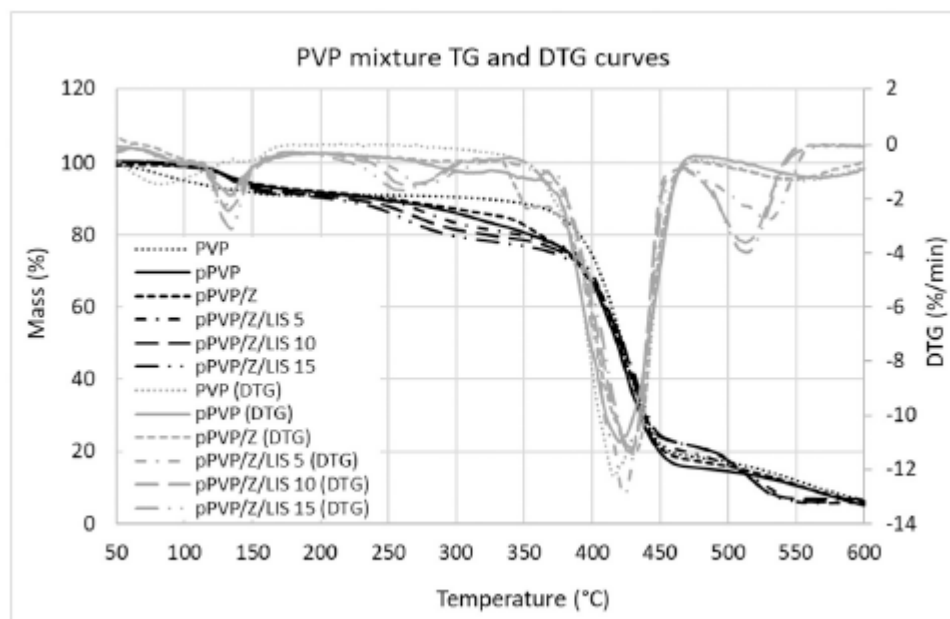


Fig. 7. TGA analysis PVP mixtures - TG and DTG curves for the cast materials of PVP, pPVP, pPVP/Z and pPVP/Z/LiS.

Table 3 TGA analysis - evaluated data on the pure additives and cast materials of PVP, pPVP, pPVP/Z and pPVP/Z/LiS.

Sample	T_{max1} (°C)	$m_{residual1}$ (%)	T_{max2} (°C)	$m_{residual2}$ (%)	T_{max3} (°C)	$m_{residual3}$ (%)	T_{max4} (°C)	$m_{residual\ total\ (\approx m_{residual4})}$ (%)
Glycerol	–	–	248	0	–	–	–	0
Zeolite	26	99	65	93	–	–	–	91
LiS	94	93	308	54	–	–	481	17
PVP	82	91	–	–	415	19	556	5
pPVP (ref.)	134	93	308	83	420	15	568	4
pPVP/Z	135	93	354	78	428	17	547	5
pPVP/Z/LiS 5	134	92	277	81	428	21	530	6
pPVP/Z/LiS 10	134	92	262	81	429	22	513	7
pPVP/Z/LiS 15	135	91	262	79	429	22	514	6

However, the last step (T_{max4}) in degradation took place earlier in blends with LiS (comparing to pPVP), as revealed by the DTG curves. On the other hand, the LiS degradation itself (T_{max4}) was moved in PVP mixtures to higher temperature from 481 °C to 514 °C for 10 and 15% LiS and to 530 °C for 5% of LiS in PVP mixture. Total residual mass was higher for mixtures with LiS than for pPVP, the greatest value being discerned for 10% LiS. General increase in total residual mass was ca 40%, hinting that LiS/ zeolite exerted a positive effect on the thermal stability of PVP [39] especially at higher temperatures.

3.5. Texture profile analysis

Hardness for pure PVP was determined as 327.4 ± 10.7 N. Plasticization of PVP by glycerol decreased this to a value of 10.9 ± 0.5 N, and the material was more flexible and softer as a consequence. This finding is in agreement with Nestic et al. [8], who stated that the physicochemical effect of the plasticizer on PVP increased its hydrophilicity, brought about through the presence of -OH groups interacting with either water or polar polymer groups; herein, it concerned the amide group from the PVP through the formation of hydrogen bonds (see the FTIR analysis). Additionally, any water bound in the system might have acted as an additional plasticizer, promoting greater elasticity of the blends. Plastification with glycerol also diminished the extent of intermolecular bonds between the PVP chains, giving rise to a softer material than pure PVP. Such plastification of PVP increased the adhesion of the material hundred times, from 0.120 ± 0.013 N (pure PVP) to 11.783 ± 2.740 N (pPVP). Although hydrogen bonds were discerned between the PVP and synthetic zeolite, addition at 2.5% of the latter had no significant effect on hardness (pPVP/Z 12.5 ± 3.3 N) or adhesion (pPVP/Z 9.137 ± 2.527 N).

As can be seen from Fig. 8, the presence of LiS in the blends had a marked effect upon hardness and adhesion. As the content of LiS increased, so did hardness in parallel with a drop in adhesion. It is believed that this effect occurred as a direct result of the strong interaction of LiS with the PVP, in addition to the inherent rigidity of the lignosulfonate structures. It would seem that supplementing the pPVP/Z mixture with LiS at 5% was optimal, halving the extent of adhesion while ensuring acceptable flexibility.

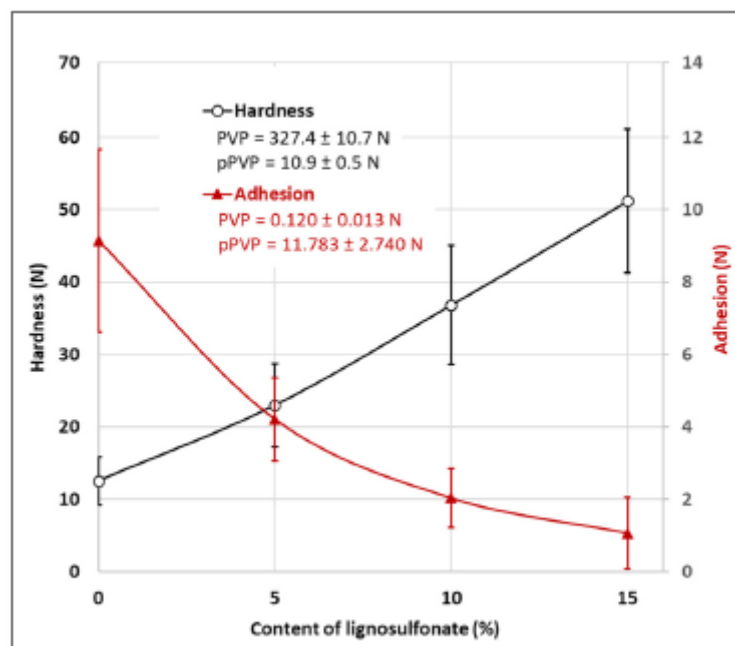


Fig. 8. Hardness and adhesion (absolute values) of the plasticized PVP with 2.5% of zeolite as a function of lignosulfonate content ($n = 15$, mean value \pm standard deviation).

3.6. Water uptake and water solubility

PVP is a hygroscopic polymer, which can be an advantage or a disadvantage depending on the intended purpose. This is a benefit when the material takes the form of a binder or adhesive, but not as a film. Water uptake and water solubility affect chemical stability and mechanical properties, thus constitute

crucial factors, alongside biodegradability, which impact practical application [53,54]. Fig. 9 illustrates the effect of lignosulfonate content on the water uptake and water solubility of the cast blends.

Water uptake for PVP was determined as $15.7 \pm 1.1\%$ at the relative humidity of 54%. The plastification of PVP and addition of zeolite both led to a decrease in water uptake of up to $3.20 \pm 0.08\%$ and $3.28 \pm 0.10\%$, respectively. This drop could be attributed to the formation of hydrogen bonds between the carbonyl group in the lactam ring and the -OH groups in the glycerol (see Fig. 4D, E), as well as hydrogen bonds between the -OH groups of zeolite and the carbonyl group or with the N atom of PVP. The highest value for water uptake was discerned for the pPVP/Z/LiS 5 blend, at $6.27 \pm 0.14\%$. As the amount of LiS went up, though, water uptake fell (10% LiS: $5.77 \pm 0.08\%$; 15% LiS: $4.26 \pm 0.17\%$). As stated in a paper by Shankar et al. [55], this reduction in water uptake might arise through the strong intermolecular force between the PVP and hydroxyl group of the aromatic polyphenolic rings in the lignosulfonate.

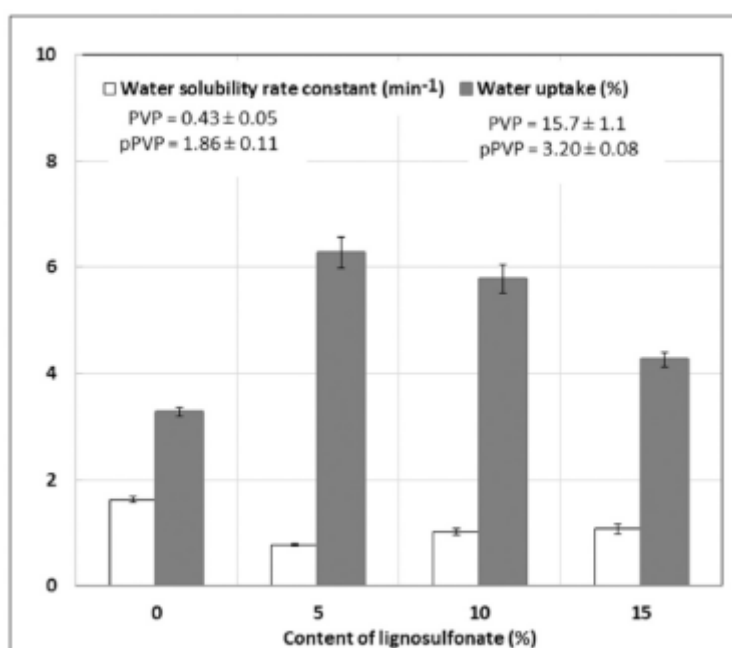


Fig. 9. Water uptake at 54% RH of the plasticized PVP with 2.5% of zeolite, as a function of lignosulfonate content after 10 days (at equilibrium), and the constant rate for water solubility as a function of lignosulfonate content ($n = 3$, mean values \pm standard deviation).

All the prepared blends were highly water soluble (100% according to COD analysis), hence a first-order mathematical model was employed to evaluate the dissolution profiles for the blends [46]. The dissolution rate, expressed as a constant for water solubility, was selected for the sake of comparison. PVP is quite soluble, and upon plastification by glycerol, the dissolution rate of the cast blend increased four-fold. After adding synthetic zeolite into the pPVP, the dissolution rate decreased from $1.86 \pm 0.11 \text{ min}^{-1}$ to $1.63 \pm 0.05 \text{ min}^{-1}$. The blends containing LiS dissolved slightly slower than the pPVP/Z blend, at $0.77 \pm 0.02 \text{ min}^{-1}$ for 5% LiS, $1.01 \pm 0.06 \text{ min}^{-1}$ for 10% LiS and $1.08 \pm 0.09 \text{ min}^{-1}$ for 15% LiS. The mass concentration of lignosulfonate exerted no statistically significant effect on the water solubility of the blends. It is known that water solubility is related to the content of free hydroxyl groups in the polymer matrix. The decrease witnessed in the dissolution rates for pPVP/Z and pPVP/Z/LiS may have occurred

through the presence of hydrogen bonding between PVP-zeolite and PVP-lignosulfonate. It could also be assumed that there was a gradual release of PVP from the porous structure of the zeolite.

The tests conducted herein led to the authors concluding that the degree of hygroscopicity of the proposed blends could be regulated by adding LiS, broadening the scope for practical application of the material.

3.7. Biodegradation and screening test on the growth of *Sinapis alba*

Experiments investigating the biodegradation of prepared cast blends with LiS in a soil environment were expected to reveal a positive effect on the biodegradation of PVP of the enzymatic apparatus (ligninolytic enzymes) formed when lignosulfonate degraded. Reference was made to the literature [56,57], wherein lignin biodegradation was reported as an oxidative process involving enzymatic and radical reactions. The free radicals of some fungal metabolites and lignin-derived products have the potential to act as natural redox mediators of ligninolytic oxidoreductases. The contribution made by these compounds would be especially noticeable in said fungi producing laccase as the main or sole ligninolytic oxidoreductase.

A respirometric test was performed for two months, and the corresponding data are presented in **Fig. 10**. The biodegradation curves adhered to a standard course, and it was possible to describe them by regression, applying an equation for first-order kinetics. A comparison of the limit values for the biodegradation of the blends is given in **Table 4**.

As expected, glycerol and lignosulfonate were highly biodegradable and pure PVP was resistant to the process ($D_{\max} < 1\%$). **Table 4** shows that the degree of biodegradation for all blends was approximately 11% and the lag phase was less than one day. However, the presence of synthetic zeolite in the blends exerted a significant effect on the rate of biodegradation. The biodegradation rate of the pPVP/Z blends almost doubled compared to pPVP, which was in agreement with Yapparov et al. [58], who wrote that zeolite improved the agrochemical properties of soil, which leads to increased microbiological activity and accelerated biomass growth of microorganisms. Adding LiS caused a reduction in the rate of biodegradation that varied depending on mass concentration, as follows: $0.244 \pm 0.010 \text{ d}^{-1}$ for 5% LiS, $0.173 \pm 0.012 \text{ d}^{-1}$ for 10% LiS and $0.183 \pm 0.012 \text{ d}^{-1}$ for 15% LiS, potentially due to the complex structure of the lignosulfonate. The findings indicated that the presence of LiS in the blends had a positive effect on biodegradation of the blends, and the optimal filling equalled a 5% mass concentration of LiS. The anticipated influence of LiS on the biodegradation of PVP proved not so significant, though. The results of biodegradation tests support the notion that the proposed pPVP/Z/LiS blends are suitable for application in a soil environment.

Finally, a plant growth test (*S. alba*) was performed to assess the applicability of the blends as seed carriers for sowing purposes (as seed tapes - Fig. 11) or as a biocompatible coating for protecting a seed, as well as possibly aiding the germination process and improving crop yield. The blend with 5% of LiS was chosen for its demonstrably good biodegradability in soil. The first positive result comprised the fact that all of the ten encapsulated seeds under study actually germinated. At the end of the experiment, the weight of the wet biomass, and the lengths of the stems and roots were determined. Wet biomass weight as control samples constituted $108.5 \pm 27.6 \text{ g}$, $105.7 \pm 22.5 \text{ g}$ for pPVP/Z and $109.1 \pm 20.1 \text{ g}$ for pPVP/Z/LiS. The length of the stems for the control samples equalled $6.0 \pm 1.0 \text{ cm}$, $7.2 \pm 0.8 \text{ cm}$ for pPVP/Z and $6.3 \pm 1.0 \text{ cm}$ for pPVP/Z/LiS. Notable results were observed for root length: control $3.7 \pm 2.5 \text{ cm}$, $1.5 \pm 0.3 \text{ cm}$ for pPVP/Z and $5.3 \pm 1.8 \text{ cm}$ for pPVP/Z/LiS. The presence of LiS in the blend brought about significant increase in the length of the roots of *Sinapis alba*, compared to

plants with seeds encapsulated in a cast blend filled solely with zeolite. Thus it could be concluded that the LiS or related biodegradation products released into the soil environment, probably humic substances, exerted a positive effect on the quality of the root system of the *Sinapis alba* plants [59,60]. Lignosulfonate may also have been a source of sulphur, which is an important element in the formation of the root system. However, it should be borne in mind that these are only screening tests and further experiments are necessary.

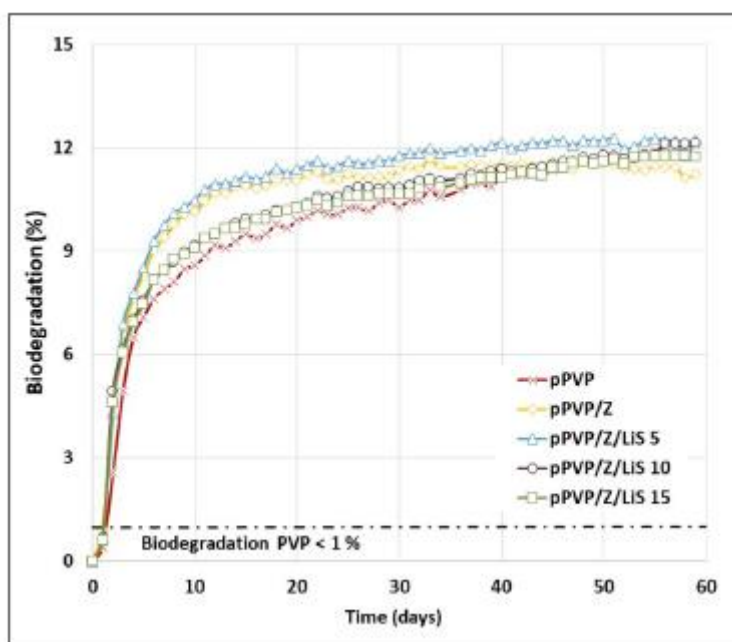


Fig. 10. Biodegradation of the cast materials of PVP, pPVP, pPVP/Z and pPVP/ Z/LiS (n = 3, mean values).

Table 4 Kinetic model parameters for the biodegradation of the cast materials of PVP, pPVP, pPVP/Z and pPVP/Z/LiS (n = 3, mean values \pm standard deviation).

Sample	D_{max} (%)	$-k$ (d^{-1})	t_{lag} (d)
PVP	< 1	–	–
pPVP	11.14 ± 0.11	0.143 ± 0.010	< 1
pPVP/Z	11.35 ± 0.04	0.260 ± 0.009	< 1
pPVP/Z/LiS 5	11.87 ± 0.06	0.244 ± 0.010	< 1
pPVP/Z/LiS 10	11.28 ± 0.10	0.173 ± 0.012	< 1
pPVP/Z/LiS 15	11.10 ± 0.09	0.183 ± 0.012	< 1

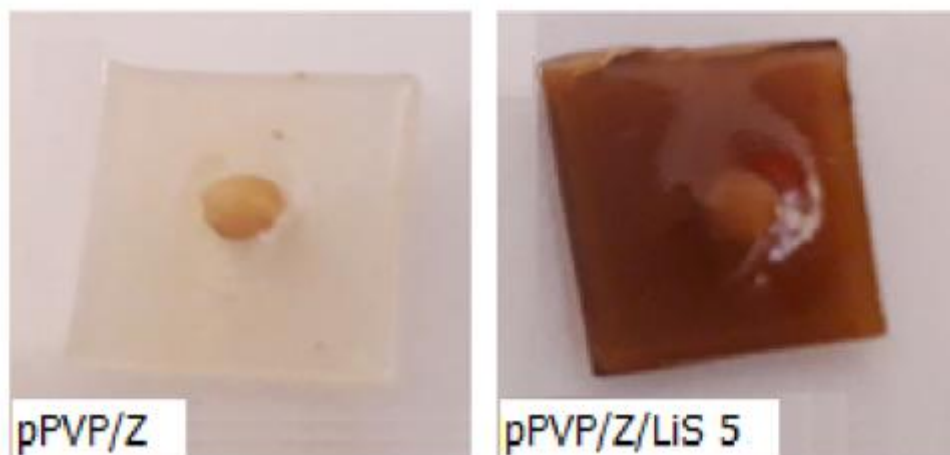


Fig. 11. Sinapis alba seeds encapsulated in the cast blends.

4. Conclusion

The present study focussed onto the development of novel ternary polymer blends based on polyvinylpyrrolidone (PVP) as the matrix with lignosulfonate and synthetic zeolite. The following conclusions are founded on the discussion given above:

- With reference to organoleptic characterization, it is clear that synthetic zeolite was necessary for preparing such cast blends on the base of PVP and LiS. Optical microscopy revealed that particles of the synthetic zeolite were quite evenly distributed throughout the polymer matrix and random networks were formed therein.
- The FTIR spectra for the prepared polymer blends proved that hydrogen-bonding interaction occurred between the PVP/synthetic zeolite and PVP/lignosulfonate.
- DSC analysis confirmed the good miscibility of the PVP and lignosulfonate.
- TGA results indicated that combining lignosulfonate and synthetic zeolite enabled the thermal stability of PVP to be maintained.
- Lignosulfonate reduced the adhesion of the polymer blends. Water solubility and water uptake was satisfactory from the point of view of handling and further use.
- Respirometric biodegradation test confirmed that the ternary polymer blends were environmentally friendly materials. The screening plant growth test demonstrated that the polymer blends had a positive effect on the root growth and development of Sinapis alba.

Optimization of the properties of PVP through blending it with synthetic zeolite and lignosulfonate is a viable, economic and good means for broadening the scope of practical application of the material. The developed ternary polymeric blends were found to be suitable for use in agricultural chemistry, for example, as seed carriers (as seed tapes) or as a biocompatible coating for protecting seeds.

References

- [1] Q.A. Acton, Polyvinyls-advances in Research And Application, Scholarly Editions, Georgia, 2013.

- [2] A. Grumezescu, *New Pesticides And Soil Sensors*, 1st. Bukurešť, 2017.
- [3] S. Chen, M. Yang, C. Ba, S. Yu, Y. Jiang, H. Zou, Y. Zhang, Preparation and characterization of slow-release fertilizer encapsulated by biochar-based waterborne copolymers, *Sci. Total Environ.* 615 (2018) 431-437, <https://doi.org/10.1016/j.scitotenv.2017.09.209>.
- [4] A. Parambath, *Engineering of Biomaterials for Drug Delivery Systems: Beyond Polyethylene Glycol*, in: Woodhead Publishing Series in Biomaterials, 1, Woodhead Publishing, an imprint of Elsevier, Duxford, United Kingdom, 2018. ISBN 978-0081017-517.
- [5] H. Soroory, A. Mashak, A. Rahimi, Application of PDMS-based coating in drug delivery systems using PVP as channeling agent, *Iran. Polym. J.* 22 (11) (2013) 791-797, <https://doi.org/10.1007/s13726-013-0178-7>.
- [6] M.W. Sulek, J. Janiszewska, K. Kurzepa, B. Mirkowska, The effect of anionic surfactant - polyvinylpyrrolidone complexes formed in aqueous solutions on physicochemical and functional properties of shampoos, *Polimery* 63 (2018) 549-556. [10.14314/polimery.2018.7.10](https://doi.org/10.14314/polimery.2018.7.10).
- [7] G. Wypych, *Handbook of Polymers*, 2nd edition, ChemTec Publishing, Toronto, 2016.
- [8] A. Nestic, J. Ružic, M. Gordic, S. Ostojic, D. Micic, A. Onjia, Pectin-polyvinylpyrrolidone films: a sustainable approach to the development of biobased packaging, *Mater.Compos.BEng.* 110 (2017) 56-61, <https://doi.org/10.1016/j.compositesb.2016.11.016>.
- [9] N.Roy N. Saha, T. Kitano, P. Saha, Biodegradation of PVP-CMC hydrogel film: a useful food packaging material, *Carbohydr. Polym.* 89 (2) (2012) 346-353, <https://doi.org/10.1016/j.carbpol.2012.03.008>.
- [10] D.A. Chalkias, D.I. Giannopoulos, E. Kollia, A. Petala, V. Kostopoulos, G. C. Papanicolaou, Preparation of polyvinylpyrrolidone-based polymer electrolytes and their application by in-situ gelation in dye-sensitized solar cells, *Electrochim. Acta* 271 (2018) 632-640, <https://doi.org/10.1016/j.electacta.2018.03.194>.
- [11] Y. Hanafi, A. Szymczyk, M. Rabiller-Baudry, K. Baddari, Degradation of poly (ether sulfone)/polyvinylpyrrolidone membranes by sodium hypochlorite: insight from advanced electrokinetic characterizations, *Environ. Sci. Technol.* 48 (22) (2014) 13419-13426, <https://doi.org/10.1021/es5027882>.
- [12] J.F. Kadla, S. Kubo, Lignin-based polymer blends: analysis of intermolecular interactions in lignin-synthetic polymer blends, *Compos.AAppl. Sci. Manuf.* 35 (3) (2004) 395-400, <https://doi.org/10.1016/j.compositesa.2003.09.019>.
- [13] M. Julinova, L. Vaňharová, M. Jurca, Water-soluble polymeric xenobiotics-polyvinyl alcohol and polyvinylpyrrolidone-and potential solutions to environmental issues: a brief review, *J. Environ. Manag.* 228 (2018) 213-222, <https://doi.org/10.1016/j.jenvman.2018.09.010>.
- [14] A. Grossman, W. Vermerris, Lignin-based polymers and nanomaterials, *Curr. Opin. Biotechnol.* 56 (2019) 112-120, <https://doi.org/10.1016/j.copbio.2018.10.009>.
- [15] A. Naseem, S. Tabasum, K.M. Zia, M. Zuber, M. Ali, A. Noreen, Lignin-derivatives based polymers, blends and composites: a review, *Int. J. Biol. Macromol.* 93 (2016) 296-313, <https://doi.org/10.1016/j.ijbiomac.2016.08.030>.

- [16] M.F. Silva, C.A. Da Silva, F.C. Fogo, E.A.G. Pineda, A.A. Hechenleitner, Thermal and FTIR study of polyvinylpyrrolidone/lignin blends, *J. Therm. Anal. Calorim.* 7 (2005) 367-370, <https://doi.org/10.1007/s10973-005-0066-2>.
- [17] K. Inna, J. Sunthornvarabhas, A. Thanapimmetha, M. Saisriyoot, P. Srinophakun, Natural antimicrobial lignin in polyvinyl alcohol and polyvinylpyrrolidone film for packaging application, *Mater. Sci. Forum* 936 (2018) 105-109, <https://doi.org/10.4028/www.scientific.net/MSF.936.105>.
- [18] D. Ye, L. Jiang, X. Hu, M. Zhang, X. Zhang, Lignosulfonate as reinforcement in polyvinyl alcohol film: mechanical properties and interaction analysis, *Int. J. Biol. Macromol.* 83 (2016) 209-215, <https://doi.org/10.1016/j.ijbiomac.2015.11.064>.
- [19] S. Kubo, J.F. Kadla, The formation of strong intermolecular interactions in immiscible blends of poly (vinyl alcohol)(PVA) and lignin, *Biomacromolecules* 4 (3) (2003) 561-567, <https://doi.org/10.1021/bm025727p>.
- [20] M. Julinová, R. Slavík, M. Vyoralová, A. Kalendová, P. Alexy, Utilization of waste lignin and hydrolysate from chromium tanned waste in blends of hot-melt extruded PVA-starch, *J. Polym. Environ.* 26 (4) (2018) 1459-1472, <https://doi.org/10.1007/s10924-017-1050-1>.
- [21] S. Wang, Y. Li, H. Xiang, Z. Zhou, T. Chang, M. Zhu, Low cost carbon fibers from bio-renewable lignin/poly (lactic acid)(PLA) blends, *Compos. Sci. Technol.* 119 (2015) 20-25, <https://doi.org/10.1016/j.compscitech.2015.09.021>.
- [22] X. Ge, M. Chang, W. Jiang, B. Zhang, R. Xing, C. Bulin, Investigation on two modification strategies for the reinforcement of biodegradable lignin/poly (lactic acid) blends, *J. Appl. Polym. Sci.* 137 (44) (2020) 49354, <https://doi.org/10.1002/app.49354>.
- [23] Y. Yan, L. Zhang, X. Zhao, S. Zhai, Q. Wang, C. Li, X. Zhang, Utilization of lignin upon successive fractionation and esterification in polylactic acid (PLA)/lignin biocomposite, *Int. J. Biol. Macromol.* (2022), <https://doi.org/10.1016/j.ijbiomac.2022.01.041>.
- [24] S.K. Samal, E.G. Fernandes, A. Corti, E. Chiellini, Bio-based polyethylene-lignin composites containing a pro-oxidant/pro-degradant additive: preparation and characterization, *Polym. Environ.* 22 (2014) 58-68, <https://doi.org/10.1007/s10924-013-0620-0>.
- [25] M.F. Silva, E.A.G. Pineda, A.A.W. Hechenleitner, D.M. Fernandes, M.K. Lima, P.R. S. Bittencourt, Characterization of poly (vinyl acetate)/sugar cane bagasse lignin blends and their photochemical degradation, *J. Therm. Anal. Calorim.* 106 (2) (2011) 407-413, <https://doi.org/10.1007/s10973-011-1475-z>.
- [26] A.C. Dos Santos, H.M. Henrique, V.L. Cardoso, M.H. Reis, Slow release fertilizer prepared with lignin and poly (vinyl acetate) bioblend, *Int. J. Biol. Macromol.* 185 (2021) 543-550, <https://doi.org/10.1016/j.ijbiomac.2021.06.169>.
- [27] E.S. Stevens, J.L. Willett, R.L. Shogren, Thermoplastic starch-kraft lignin-glycerol blends, *J. Biobased Mater. Bioenergy* 1 (3) (2007) 351-359, <https://doi.org/10.1166/jbmb.2007.009>.
- [28] S.M. Auerbach, K.A. Carrado, P.K. Dutta, *Handbook of Zeolite Science And Technology* 1, M. Dekker, New York, 2003.
- [29] K. Ramasubramanian, M.A. Severance, P.K. Dutta, W.W. Ho, Fabrication of zeolite/ polymer multilayer composite membranes for carbon dioxide capture: deposition of zeolite particles on

polymer supports, *J. Colloid Interface Sci.* 452 (2015) 203-214, <https://doi.org/10.1016/j.jcis.2015.04.014>.

[30] U. Habiba, T.A. Siddique, T.C. Joo, A. Salleh, B.C. Ang, A.M. Afifi, Synthesis of chitosan/polyvinyl alcohol/zeolite composite for removal of methyl orange, Congo Red and chromium(vi) by flocculation/adsorption, *Carbohydr. Polym.* 157 (2017) 1568-1576, <https://doi.org/10.1016/j.carbpol.2016.11.037>.

[31] K.Z. Elwakeel, A.A. El-Bindary, E.Y. Kouta, E. Guibal, Functionalization of polyacrylonitrile/Na-Y-zeolite composite with amidoxime groups for the sorption of Cu(II), Cd (II) and Pb(II) metal ions, *Chem. Eng. J.* 332 (2018) 727-736, <https://doi.org/10.1016/j.cej.2017.09.091>.

[32] G. Zhao, Y. Sheng, C. Wang, J. Yang, Q. Wang, L. Chen, In situ microbial remediation of crude oil-soaked marine sediments using zeolite carrier with a polymer coating, *Mar. Pollut. Bull.* 129 (1) (2018) 172-178, <https://doi.org/10.1016/j.marpolbul.2018.02.030>.

[33] F.U. Nigiz, S. Veli, N.D. Hilmioglu, Deep purification of seawater using a novel zeolite 3A incorporated polyether-block-amide composite membrane, *Sep. Purif. Technol.* 188 (2017) 90-97, <https://doi.org/10.1016/j.seppur.2017.07.017>.

[34] A. Nestic, S. Meseldzija, G. Cabrera-Barjas, A. Onjia, Novel biocomposite films based on high methoxyl pectin reinforced with zeolite Y for food packaging applications, *Foods* 11 (3) (2022) 360, <https://doi.org/10.3390/foods11030360>.

[35] V.P. Babu, W.J. Koros, The role of polyvinylpyrrolidone in forming open-porous, macrovoid-free mixed matrix sorbents from Torlon®, a polyamide-imide polymer, *Polym. Eng. Sci.* 58 (11) (2018) 2106-2114, <https://doi.org/10.1002/pen.24823>. ISSN 00323888.

[36] F.N. Tanaka, C.R. Ferreira Jr., M.R. de Moura, F.A. Aouada, Water absorption and physicochemical characterization of novel zeolite-PMAA-co-PAAm nanocomposites, *J. Nanosci. Nanotechnol.* 18 (10) (2018) 7286-7295, <https://doi.org/10.1166/jnn.2018.15515>.

[37] B.I. Kharisov, O.V. Kharisova, V. Ortiz-Mendes, *Encyclopedia of Nanotechnology 1*, CRC Press Taylor and Francis Group, London, 2016.

[38] G. Venkatesulu, P.K. Babu, Y. Maruthi, C. Madhavi, A. Parandhama, M.C.S. Subha, K.C. Rao, Design and application of H-ZSM-5 zeolite loaded hydroxy propyl cellulose/poly(vinyl pyrrolidone) mixed matrix membranes for dehydration of ethanol by pervaporation, *Indian J. Adv. Chem. Sci.* 4 (4) (2016) 496-505.

[39] E. Alver, A.U. Metin, H. ifti, Synthesis and characterization of chitosan/polyvinylpyrrolidone/zeolite composite by solution blending method, *J. Inorg. Organomet. Polym.* 24 (6) (2014) 1048-1054, <https://doi.org/10.1007/s10904-014-0087-z>.

[40] E.I. da Silva Oliveira, J.B. Santos, S. Mattedi, N.M. Jose, Rambutan peel: an unconventional source of lignin and its potential applications in polymer science, *Res. Soc. Dev.* 11 (1) (2022), <https://doi.org/10.33448/rsd-v11i1.25320> e49911125320-e49911125320.

[41] N. Mazloom, R. Khorassani, G.H. Zohury, H. Emami, J. Whalen, Lignin-based hydrogel alleviates drought stress in maize, *Environ. Exp. Bot.* 175 (2020), 104055, <https://doi.org/10.1016/j.envexpbot.2020.104055>.

- [42] V. Krishnamoorthy, G. Elumalai, S. Rajiv, Environment friendly synthesis of polyvinylpyrrolidone nanofibers and their potential use as seed coats, *New J. Chem.* 40 (4) (2016) 3268-3276, <https://doi.org/10.1039/C5NJ03008K>.
- [43] M.K. Naskar, D. Kundu, M. Chatterjee, Influence of PVP buffer layer on the formation of NaA zeolite membrane, *J. Porous. Mater.* 18 (2011) 319-327, <https://doi.org/10.1007/s10934-010-9381-5>.
- [44] L. Vanharová, M. Julinová, M. Jurca, A. Minarík, S. Vinter, D. Sasinková, E. Wrzecionko, Environmentally friendly polymeric films based on biocarbon, synthetic zeolite and PVP for agricultural chemistry, *Polym. Bull.* (2021) 1-28, <https://doi.org/10.1007/s00289-021-03765-z>.
- [45] ISO 15705, Water Quality - Determination of the Chemical Oxygen Demand -Small-scale Dealer-tube Method, 2002.
- [46] P. Costa, J.M.S. Lobo, Modeling and comparison of dissolution profiles, *Eur. J. Pharm. Sci.* 13 (2) (2001) 123-133, [https://doi.org/10.1016/S0928-0987\(01\)00095-1](https://doi.org/10.1016/S0928-0987(01)00095-1).
- [47] P. Pitter, J. Chudoba, Biodegradability of Organic Substance in the Aquatic Environment, CRC Press, Boca Raton, 1990.
- [48] ISO 11269-2, Soil quality - determination of the effects of pollutants on soil flora -part 2: effects of chemicals on the emergence and growth of higher plants, 2013.
- [49] O. Orliac, A. Rouilly, F. Silvestre, L. Rigal, Effects of various plasticizers on the mechanical properties, water resistance and aging of thermo-moulded films made from sunflower proteins, *Ind. Crops Prod.* 18 (2) (2003) 91-100, [https://doi.org/10.1016/S0926-6690\(03\)00015-3](https://doi.org/10.1016/S0926-6690(03)00015-3).
- [50] V. Belyy, I. Kuzivanov, E. Istomina, V. Mikhaylov, E. Tropnikov, A. Karmanov, N. Bogdanovich, Water stable colloidal lignin-PVP particles prepared by electrospray, *Int. J. Biol. Macromol.* 190 (2021) 533-542, <https://doi.org/10.1016/j.ijbiomac.2021.09.013>.
- [51] J. Kubacková, J. Feranc, I. Hudec, S. Sutý, M. Jablonský, J. Annus, J. Preťo, Antioxidant properties of lignin in rubber blends, *Elastomery* 17 (3) (2013) 21-27.
- [52] Y. Liu, C. Yan, J. Zhao, Z. Zhang, H. Wang, S. Zhou, L. Wu, Synthesis of zeolite P1 from fly ash under solvent-free conditions ammonium removal from water, *J. Clean. Prod.* 202 (2018) 11-22, <https://doi.org/10.1016/j.jclepro.2018.08.128>.
- [53] G.M. Bennet, Seed Inoculation, Coating And Precision Pelleting: Science Technology And Practical Applications, CRC Press, USA, 2016.
- [54] R.S. Meena, A. Das, G.S. Yadav, R. Lal, Legumes for Soil Health And Sustainable Management, Springer, India, 2018.
- [55] S. Shankar, J.P. Reddy, J.W. Rhim, Effect of lignin on water vapor barrier, mechanical, and structural properties of agar/lignin composite films, *Int. J. Biol. Macromol.* 81 (2015) 267-273, <https://doi.org/10.1016/j.ijbiomac.2015.08.015>.
- [56] M. Julinová, J. Kupec, P. Alexy, J. Hoffmann, V. Sedlarík, T. Vojtek, J. Chromcáková, P. Bugaj, Lignin and starch as potential inductors for biodegradation of films based on poly(vinyl alcohol) and protein hydrolysate, *Polym. Degrad. Stabil.* 95 (2) (2010) 225-233, <https://doi.org/10.1016/j.polymdegradstab.2009.10.008>.

- [57] A.I. Canas, M. Alcalde, F. Plou, M.J. Martinez, A.T. Martinez, S. Camarero, Transformation of polycyclic aromatic hydrocarbons by laccase is strongly enhanced by phenolic compounds present in soil, *Environ. Sci. Technol.* 41 (8) (2007) 2964-2971, <https://doi.org/10.1021/es062328j>.
- [58] A.K. Yapparov, L.K. Bikkinina, I.A. Yapparov, S.A. Aliev, A.M. Ezhkova, V. O. Ezhkov, R.R. Gazizov, Changes in the properties and productivity of leached chernozem and gray forest soil under the impact of ameliorants, *Eurasian Soil Sci.* 48 (2015) 1149-1158, <https://doi.org/10.1134/S1064229315100130>.
- [59] A. Dursun, I. Guvenç, M. Turan, Effects of different levels of humic acid on seedling growth and macro and micronutrient contents of tomato and eggplant, *Acta Agrobot.* 55 (2) (2002) 81-88, <https://doi.org/10.5586/aa.2002.046>.
- [60] O. Turkmen, A. Dursun, M. Turan, ę. Erdineę, Calcium and humic acid affect seed germination, growth, and nutrient content of tomato (*Lycopersicon esculentum* L.) seedlings under saline soil conditions, *Acta Agric. Scand. Sect. B-Soil Plant Sci.* 54 (3) (2004) 168-174, <https://doi.org/10.1080/09064710310022014>.